J Therm Anal Calorim (2011) 104:949–954
DOI 10.1007/s10973-011-1319-x

Effect of s-, p-, d-, and f-block elements on the structure and properties of ammonium dihydrogen phosphate crystals

M. Amutha · G. Ramasamy · S. P. Meenakshisundaram · S. C. Mojumdar

CTAS2010 Conference Special Chapter
© Akadémiai Kiadó, Budapest, Hungary 2011

Abstract The influence of the s-, p-, d-, and f-block elements (Cs, Sb, Pd, and Ce) doping on the properties of ammonium dihydrogen phosphate (ADP) crystals has been described. Incorporation of small quantity of dopants into the crystalline matrix is well confirmed by energy dispersive X-ray spectroscopy (EDS) and inductively coupled plasma (ICP) techniques. The reduction in the intensity observed in powder X-ray diffraction (XRD) of doped specimens and slight shifts in vibrational frequencies confirm the lattice stress. Surface morphological changes due to doping of metals are observed by scanning electron microscopy (SEM). The differential scanning calorimetry (DSC) curves show only a slight variation in endothermic peak temperatures. The sharpness of the DSC peaks shows the good degree of crystallinity of the material. The cell parameters have been determined using single crystal XRD analysis of pure ADP and ADP:Cs/ADP:Sb/ADP:Pd/ADP:Ce specimens. The influence of metals on the second harmonic generation (SHG) efficiency is also investigated.

M. Amutha · G. Ramasamy · S. P. Meenakshisundaram
Department of Chemistry, Annamalai University, Annamalainagar 608002, India

S. C. Mojumdar
University of New Brunswick, Fredericton, NB E3B 5A3, Canada

S. C. Mojumdar (✉)
Department of Chemical and Biochemical Engineering, The University of Western Ontario, London, ON N6A 5B9, Canada
e-mail: scmojumdar@yahoo.com

S. C. Mojumdar
Department of Chemical Technologies and Environment, Faculty of Industrial Technologies, Trenčín University, 020 32 Púchov, Slovakia

Keywords Ammonium dihydrogen phosphate · Nonlinear optical properties · Doping · DSC · XRD · SEM

Introduction

Ammonium dihrdogen phosphate crystals are widely used as the second, third, and fourth hormonic generator for Nd:YAG and Nd:YLF lasers. It belongs to the tetragonal system with the space group 1-42d [1]. These crystals are widely used for electro-optical applications such as Q-switching for Ti–sapphire and alexandrite lasers as well as for acousto-optical applications [2–4]. Single crystals of ADP are used for frequency doubling and tripling of laser systems [2].

The effect of doping metal ions Cr^{3+}, Fe^{3+}, and Al^{3+} on ADP crystals has been studied elaborately in the past few years [5–7]. Recently, we have investigated the effect of KCl doping on ADP specimens in detail and the studies reveal that the dopant KCl predominantly occupies the interstitial positions of ADP crystal [8, 9]. The effect of metal doping on the physical and NLO properties of KHP and ZTS crystals are studied in detail [10–15]. We have also proved the influence of organic complexing agents and chelating agents on ADP, KHP, and ZTS crystals [16–18]. It was inferred that the cationic substitution on crystal lattice influences the lattice parameters, XRD intensities, crystallite size, effective particle size, changes in FT-IR spectral peaks, morphology, and SHG conversion efficiency [19]. The partial anionic substitution of AsO_4^{3-} for PO_4^{3-} in ADP increases the Curie temperature from 148 to 198 K [20]. Hence, it is clear that the partial substitution of anion or cation resulting in the formation of crystal defects on the host framework causes the changes in the physical properties of the parent compound. In the present investigations, we are comparing the effect of doping the s-, p-, d-, and f-block metal ions [Cs(I), Sb(III),

Pd(II), and Ce(IV)] on the lattice constants, XRD intensity, crystallite size, vibrational patterns, EDS, morphology, thermal, and SHG conversion efficiency of ADP crystal.

Experimental

Synthesis and crystal growth

ADP (E. Merck) was purified by repeated recrystallization. The crystals were grown by slow evaporation solution growth technique (SEST). A saturated aqueous solution of ADP was prepared. 1 mol% of the dopants, Cs(I) in the form of CsCl, Sb(III) in the form of $SbCl_3$, Pd(II) in the form of $PdCl_2$, and Ce(IV) as $Ce(NH_4)_2(NO_3)_6$ were added in the growth medium. The seed crystals are allowed to float on the surface of the saturated solution and left for slow evaporation at room temperature (30 °C). Triply distilled water was used as solvent. The prepared solution was filtered with a micro filter. The crystallization took place within 10–20 days and the crystals were harvested when they attained an optimal size and shape. Bulk crystals are grown using optimized growth parameters. High quality transparent crystals were harvested from the growth medium. Photographs of the as-grown crystals are shown in Fig. 1.

Measurements

The FT-IR spectra were recorded on an AVATAR 330 FT-IR by KBr pellet technique.

Bruker AXS (Kappa Apex II) X-ray diffractometer was used for single crystal XRD studies in the 2θ range of 0°–100°.

Morphologies of the samples and the presence of dopants in the specimens were observed using a JEOL JSM 5610 LV scanning electron microscope with the resolution of 3.0 nm, an accelerating voltage of 20 kV and maximum magnification 300,000 times.

The second harmonic generation test on the crystals was performed by the Kurtz powder SHG method [21]. An Nd:YAG laser with modulated radiation of 1064 nm was used as the optical source and directed on the powdered sample through a filter. The grown crystals were ground to a uniform particle size of 125–150 μm and then packed in a micro capillary of uniform bore and exposed to laser radiation. The output from the sample was monochromated to collect the intensity of the 532 nm component and to eliminate the fundamental. ICP studies were recorded by using Optima 5000 DV series spectrometer.

DSC curves were recorded on a DSC-60 Shimadzu analyzer simultaneously obtained in nitrogen atmosphere at a heating rate of 20 °C/min.

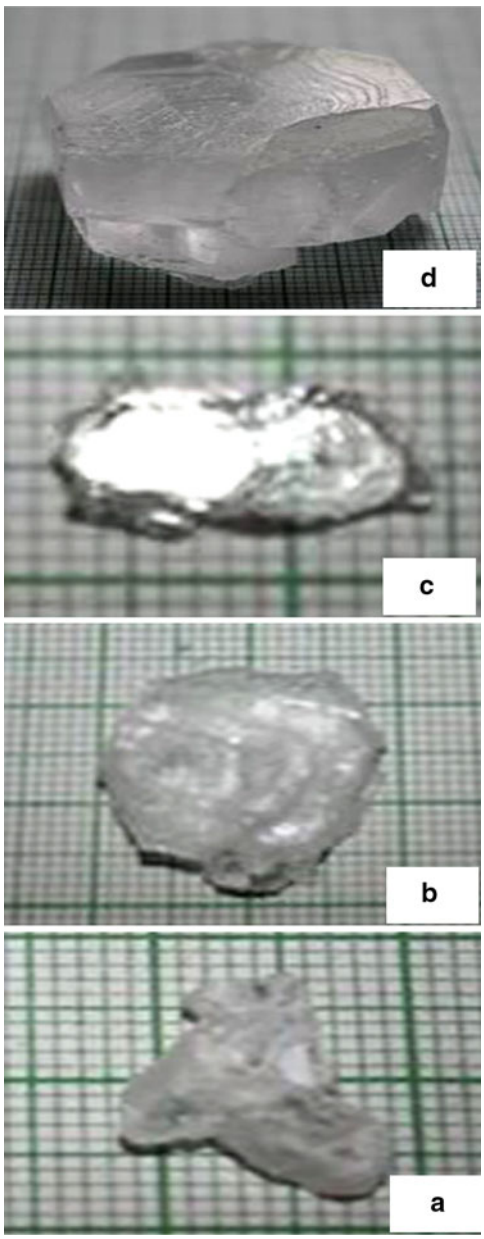

Fig. 1 Photographs of as-grown crystals, **a** ADP:Cs, **b** ADP:Sb, **c** ADP:Pd, **d** ADP:Ce

Results and discussion

FT-IR analysis

A very slight shift in some of the characteristic vibrational frequencies of pure ADP is observed because of doping with s-, p-, d-, and f-block metals. It could be due to the lattice strain developed as a result of doping (Fig. 2). Some characteristic frequencies are given in Table 1.

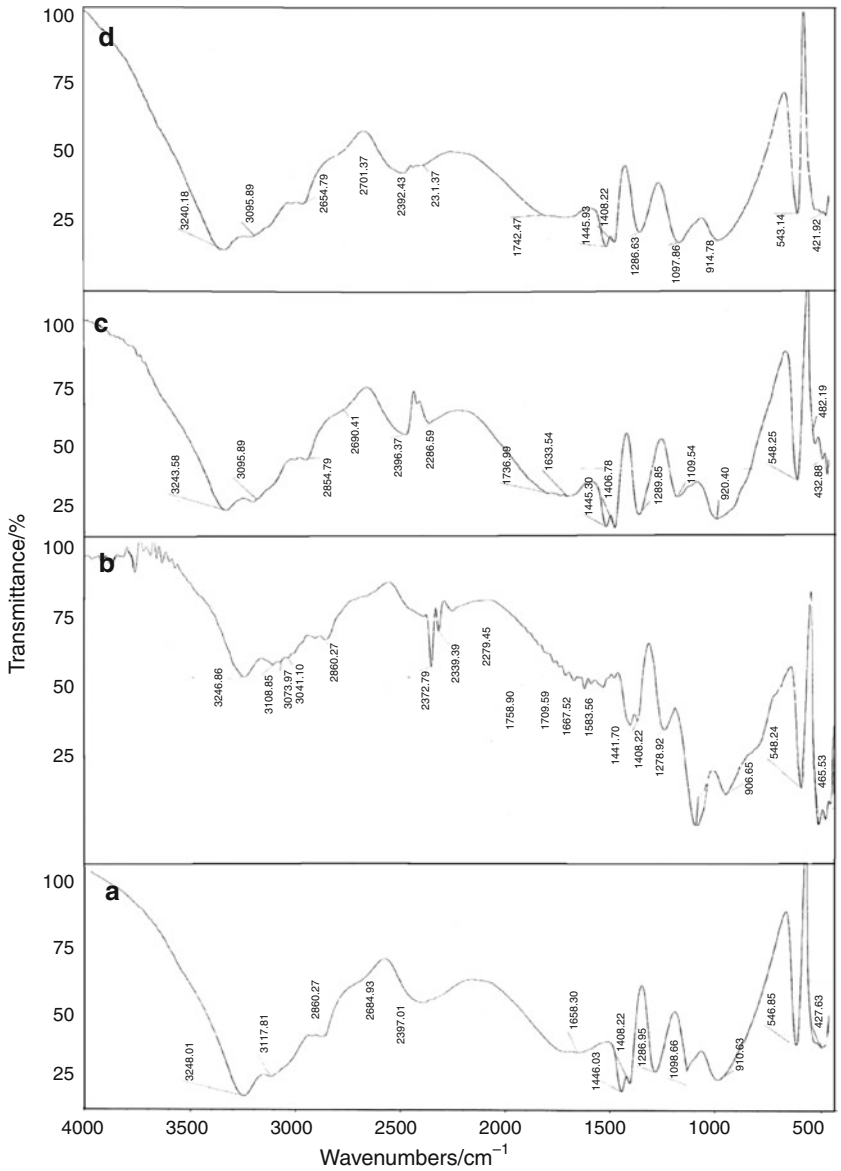

Fig. 2 FTIR spectra of crystals, **a** ADP:Cs, **b** ADP:Sb, **c** ADP:Pd, **d** ADP:Ce

Table 1 FTIR frequencies of fundamental vibrations of pure ADP and doped samples/cm^{-1}

	ADP	ADP:Cs	ADP:Sb	ADP:Pd	ADP:Ce
PO_4 stretching	1092	1098	1097	1109	1097
	932	910.63	906.65	920	914
PO_4 bending	470	427.63	465.53	482.19	421
	544	546.85	548.24	548.25	548.21
–NH_4 stretching	1402	1408.22	1408.22	1405.78	1408
–OH bending	1292	1286.95	1278.92	1289.85	1286.63
N–H–O stretching	3200	3246.01	3246.86	3243.56	3240
		3117.81	3106.85	3095.81	3095.89

XRD analysis

XRD analysis of pure and doped crystals is shown in Fig. 3. There are some changes in peak intensities and slight shifts in peak positions. The cell parameters have been determined by single crystal XRD analysis for pure and metals doped ADP crystals. These values are close to the corresponding JCPDS values (76-0414) for pure ADP with very nominal changes

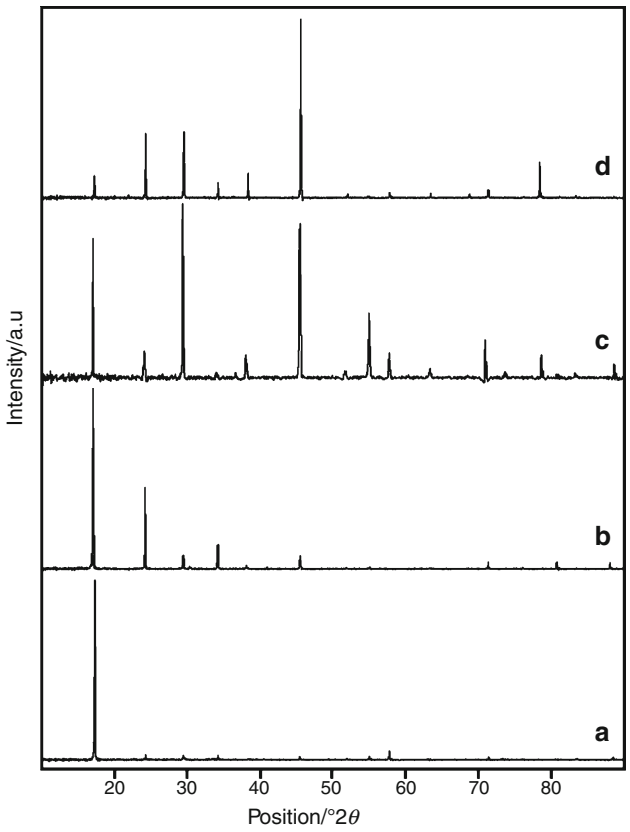

Fig. 3 Powder XRD patterns of crystals, **a** ADP:Cs, **b** ADP:Sb, **c** ADP:Pd, **d** ADP:Ce

due to doping. The values of the lattice constants of pure ADP and metal doped ADP crystals are given in Table 2.

The crystallite sizes (t) are calculated using the Scherrer equation:

$$t = \kappa\lambda/\beta\cos\theta$$

where κ is Scherrer constant, λ is the wavelength of X-ray, θ is the peak position measured in radian, and β is the integral breadth of reflections (in radians 2θ) located at 2θ. The crystallite sizes depend on the nature of the dopant (Table 2).

The changes in peak intensities, peak shifts in the XRDs and the meager increase in lattice parameters could be attributed to the strain developed by the incorporation of dopants. Further studies are required to establish the position occupancy of the dopants in the host crystalline matrix.

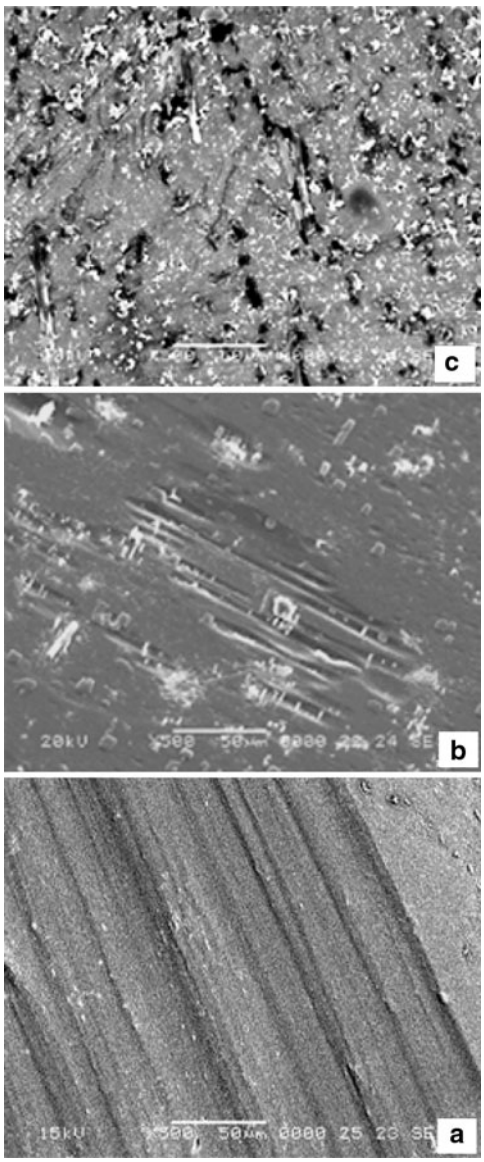

Fig. 4 SEM images of crystals, **a** pure, **b** ADP:Pd, **c** ADP:Ce

SEM and EDS analyses

The investigation of the influence of metal ions of Pd and Ce doping on the surface morphology of ADP crystal faces reveals the formation of structure defect centers. The incorporation of metals in the crystalline matrix results in

Table 2 Values of lattice constants a, b, c, cell volume V, and crystallite size

Crystal	$a = b$/Å	c/Å	Cell volume/Å^3	Cryst. size/nm	System
ADP (JCPDS 76-0414)	7.5024 (±0.0004)	7.566 (±0.0004)	428.6	–	Tetragonal
ADP:Cs	7.5120 (±0.0011)	7.5592 (±0.0011)	426.56	78.79	Tetragonal
ADP:Sb	7.5068 (±0.0004)	7.5564 (±0.0004)	425.87	88.99	Tetragonal
ADP:Pd	7.5080 (±0.0006)	7.5580 (±0.0006)	426.04	68.185	Tetragonal
ADP:Ce	7.5100 (±0.0008)	7.5564 (±0.0008)	426.18	60.50	Tetragonal

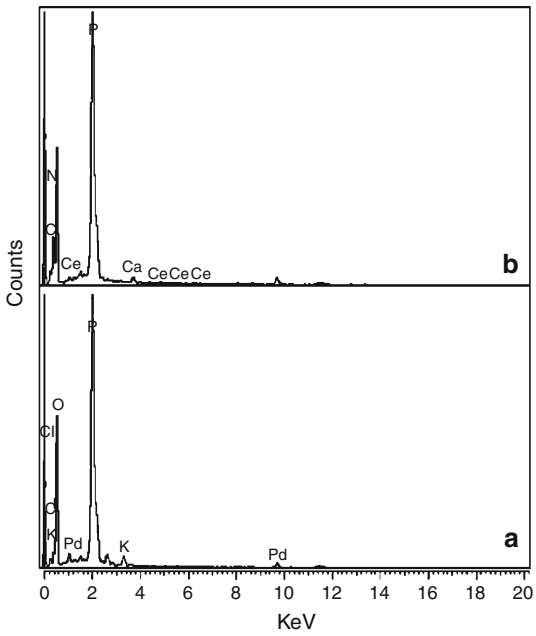

Fig. 5 EDS spectra of crystals, **a** ADP:Pd, **b** ADP:Ce

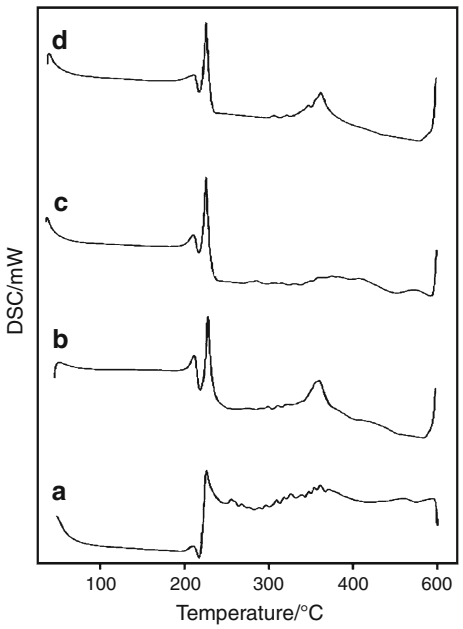

Fig. 6 DSC curves of crystals, **a** ADP:Cs, **b** ADP:Sb, **c** ADP:Pd, **d** ADP:Ce

more voids and scatter centers than that of pure ADP crystal (Fig. 4).

The incorporation of metals into the crystalline matrix was confirmed by EDS performed on ADP (Fig. 5). It is observed that the accommodating capability of the host ADP is limited and only a very small quantity of the dopant is incorporated into the ADP crystalline matrix.

ICP analysis

The amounts of respective dopant in doped ADP crystals are determined using ICP. The metal ion incorporation is small but significant. The Ce(IV) and Pd(II) incorporation (1.44 and 0.95 ppm, respectively) into the ADP crystalline matrix is appreciable compared to the small quantity of incorporation in the case of Sb(III) (0.30 ppm). Interestingly, Cs(I) incorporation is almost negligible (0.15 ppm) and this is justified since the radius of Cs(I) is high (181 pm) compared to NH_4^+ (151 pm) and other p-, d-, and f-block elements used in this study [90, 100, and 101 ppm, respectively, for Sb(III), Pd(II), and Ce(IV)].

DSC analysis

Thermal parameters are not affected much by doping (Fig. 6). The investigation shows that there is no physically adsorbed water in the molecular structure of pure and doped crystals. The sharpness of the DSC peaks shows the good degree of crystallinity of the material. No decomposition up to the melting point ensures the stability of the material for application in laser where the crystals are required to withstand high temperatures. The sharp endothermic peak is indicative of solid state transition for relatively pure material (Fig. 6).

Table 3 SHG outputs

System	$I_{2\omega}$/mV
ADP	31
ADP:Cs	37
ADP:Sb	32
ADP:Ce	35
ADP:Pd	34

SHG efficiency

In order to confirm the influence of metal doping on the NLO properties, the pure and doped crystals were subjected to SHG test with an input radiation at 3.14 mJ/pulse. The output SHG intensities of pure and doped specimens give the relative NLO efficiencies of the measured specimens. It is clearly seen from Table 3 that doping has some moderate influence on the NLO properties of ADP crystals.

Conclusions

We have used XRD, FTIR, SEM, EDS, ICP, DSC, and Kurtz powder techniques to study the influence of doping with s-, p-, d-, and f-block elements on ADP crystals. Some

minor variations in XRD and FTIR reveal that the crystal undergoes considerable lattice stress as a result of doping. SEM images reveal that the external morphology of ADP crystal depends on the nature of the dopant. EDS and ICP analysis confirm the incorporation of metals into the host crystalline matrix. Instead of small quantity metal incorporation in ADP matrix, there is no appreciable change in the cell parameter values. The DSC studies reveal the purity of the material and no decomposition is observed up to the melting point. Doping of elements of s-, p-, d-, and f-block slightly improves the SHG efficiency.

References

1. Mcmurdie H, Morris M, Evans E, Peretzkin B, Wong-Ng W, Zhang Y. Standard X-ray diffraction powder patterns from the JCPDS research associateship. Powder Diffr. 1986;1:335–45.
2. Zaitseva N, Carman L. Rapid growth of KDP-type crystals. Prog Cryst Growth Charact. 2001;43:1–118.
3. Klimentov SM, Garnov SV, Epifanov AS, Manenkov AA. Transient photoconductivity spectroscopy of poly crystalline diamond films. Prog SPIE. 1994;2145:342–54.
4. Ramirez R, Gonzala JA. Comparative analysis of the anti ferro electric behavior in $C_4O_4H_2$ and $NH_4H_2PO_4$. Solid State Commun. 1990;75:482–91.
5. Loiacono GM, Zola JJ, Kostecky G. The taper effect in KH_2PO_4 type crystals. J Cryst Growth. 1982;58:495–9.
6. Alexandru HV. Solution growth: industrial, biological and molecular crystallization, growth kinetics of prismatic faces of ammonium dihydrogen phosphate crystal in solutions. J Cryst Growth. 1996;169:347–54.
7. Davey RJ, Mullin JW. A mechanism for the habit modification of ammonium dihydrogen phosphate crystals. Krist Technol. 1976; 11:229–33.
8. Bhagavannarayana G, Parthiban S, Meenakshisundaram S. An interesting correlation between crystalline perfection and second harmonic generation efficiency on KCl- and oxalic acid doped ADP crystal. Cryst Growth Des. 2008;8:446–51.
9. Meenakshisundaram S, Parthiban S, Madhurambal G, Mojumdar SC. Effect of low and high concentrations of KCl dopant on ADP crystal properties. J Therm Anal Calorim. 2009;96:77–80.
10. Parthiban S, Murali S, Madhurambal G, Meenakshisundaram SP, Mojumdar SC. Effect of zinc(II) doping on thermal and optical properties of potassium hydrogen phthalate (KHP) crystals. J Therm Anal Calorim. 2010;100:751–6.
11. Ramasamy G, Parthiban S, Meenakshisundaram SP, Mojumdar SC. Influence of alkali metal sodium doping on the properties of potassium hydrogen phthalate (KHP) crystals. J Therm Anal Calorim. 2010;100:861–5.
12. Muthu K, Bhagvannarayanna G, Chandrasekaran C, Parthiban S, Meenakshisundaram SP, Mojumdar SC. Os(VIII) doping effects on the properties and crystalline perfection of potassium hydrogen phthalate (KHP) crystals. J Therm Anal Calorim. 2010;100:793–9.
13. Bhagavannarayana G, Kushwaha SK, Parthiban S, Meenakshisundaram S. The influence of Mn-doping on the nonlinear optical properties and crystalline perfection of tris(thiourea) zinc(II) sulphate crystals: concentration effect. J Cryst Growth. 2009;311:960–5.
14. Kasthuri L, Bhagavannarayana G, Parthiban S, Ramasamy G, Muthu K, Meenakshisundaram S. Rare earth cerium doping effects in nonlinear optical materials: potassium hydrogen phthalate (KHP) and tris(thiourea) zinc(II) sulphate (ZTS). Cryst Eng Commun. 2010;12:493–9.
15. Bhagavannarayana G, Parthiban S, Chandrasekaran C, Meenakshisundaram S. Effect of alkaline earth and transition metals doping on the properties and crystalline perfection of potassium hydrogen phthalate (KHP) crystals. Cryst Eng Commun. 2009;11:1635–41.
16. Meenakshisundaram SP, Parthiban S, Madhurambal G, Dhanasekaran R, Mojumdar SC. Effect of complexing agemt (1,10-phenanthroline) on ADP and KDP crystals. J Therm Anal Calorim. 2008;94:15–20.
17. Meenakshisundaram SP, Parthiban S, Madhurambal G, Mojumdar SC. Effect of chelating agent (1,10-phenanthroline) on potassium hydrogen phthalate crystals. J Therm Anal Calorim. 2008;94:21–5.
18. Meenakshisundaram SP, Parthiban S, Kalavathy R, Madhurambal G, Bhagavannarayana G, Mojumdar SC. Thermal and optical properties of ZTS single crystals in the presence of 1,10-phenanthroline (Phen). J Therm Anal Calorim. 2010;100:831–7.
19. Parthiban S. Crystal growth and characterisation of some nonlinear optical (NLO) materials. PhD Thesis, Department of Chemistry, Annamalai University, Annamalai Nagar, India, 2009.
20. Naili H, Mhiri T, Daoud A. Structural, vibrational and calorimetric study of a new ammonium dihydrogen phosphate-arsenate: $NH_4H_2(PO_4)_{0.52}(AsO_4)_{0.48}$. Int J Inorg Mater. 2001;4:393–400.
21. Kurtz SK, Perry TT. A powder technique for the evaluation of nonlinear optical materials. J Appl Phys. 1968;39:3798–813.